

Isoniazid loaded gelatin-cellulose whiskers nanoparticles for controlled drug delivery applications

MANDIP SARMAH^a, ANOWAR HUSSAIN^b, ANAND RAMTEKE^b and TARUN K MAJI^{a,*}

^aDepartment of Chemical Sciences, Tezpur University, Tezpur, Assam, 784 028, India

^bDepartment of Molecular Biology and Biotechnology, Tezpur University, Tezpur, Assam, 784 028, India
e-mail: tkm@tezu.ernet.in

MS received 9 March 2016; revised 15 June 2016; accepted 15 June 2016

Abstract. Natural polymers like gelatin have been used as a potential drug carrier for controlled delivery applications due to their various advantages over synthetic polymers. Cellulose Whiskers (CWs) have the capacity to form strong hydrogen bonds which help in controlling the release of drug and also provide good strength to the drug carrier. In this report, CWs were prepared from filter paper cellulose by acid hydrolysis. Also, attempt was made to prepare gelatin-CWs nanoparticles by desolvation method using an anti-tuberculosis drug, isoniazid and a crosslinker glutaraldehyde (GA). The CWs and gelatin-CWs nanoparticles were characterized by X-ray diffractometry (XRD), Fourier Transform Infrared Spectroscopy (FTIR), Scanning Electron Microscopy (SEM) and Transmission Electron Microscopy (TEM). The effect of CWs on gelatin nanoparticles over 8-hour period was measured in swelling studies. Efficiency of drug loading and subsequent release of isoniazid in buffer solutions at pH 1.2 (0.1N HCl) and pH 7.4 (phosphate buffer) were studied. Cytotoxicity study showed less toxicity for gelatin-CWs nanoparticles.

Keywords. Controlled drug delivery; isoniazid; gelatin nanoparticles; cellulose whiskers; glutaraldehyde.

1. Introduction

Controlled drug delivery system represents one of the most advancing areas of science in recent times. This system has numerous advantages including reduced toxicity, improved efficacy and convenience.¹ Nowadays, biodegradable polymers find widespread use in drug delivery due to their degradation inside the body. They also have various advantages over the synthetic polymers including biocompatibility, non-toxicity, free availability and eco-friendly nature.^{2,3}

Gelatin is a type of biodegradable and non-toxic polymer which can readily be used as a potential drug carrier for controlled delivery purposes. It is a high molecular weight amphoteric protein derived from animal collagen by alkaline or acidic pretreatment and positively charged below its isoelectric point. It bears multiple modification prospects for coupling with targeting-ligands, crosslinkers, and also shielding substances due to their intrinsic protein structure with different functional groups. Also, the hydrophilicity of gelatin is predictable to assist the fluid penetration into the particles and, thereby improve the diffusion-mediated drug release.^{4,5}

Cellulose whiskers (CWs) are rod-like crystals obtained by acid hydrolysis of cellulose fibers. The

dimension and properties of CWs vary depending on the sources and the hydrolysis conditions employed.⁶ Recently, they have gained much attention as a favorable material in pharmaceutical applications mainly due to their good mechanical properties and properties like hydrophilicity, biodegradability and high surface area. CWs consist of slender parallelepiped rods with nanometric dimensions having very high tensile modulus and good renewable character. They are mainly used as reinforcing fillers in several types of polymeric matrices in aqueous suspension giving rise to very tough percolating networks of hydrogen bonded whiskers.⁷⁻⁹ However, much research has not been done with CWs in the field of controlled drug delivery.

Isoniazid, an anti-tuberculosis drug, has been used as a model drug for controlled delivery applications.¹⁰ In recent days, emphasis is given to prepare nanoparticles for the controlled delivery of different active agents or drugs such as proteins, genes, peptides, etc.¹¹⁻¹³ Nanoparticles can be prepared from different natural biodegradable polymers, polysaccharides, proteins, etc. Gelatin nanoparticles can be prepared by using desolvation method and thus eliminating the use of toxic organic solvents.¹⁴ The use of gelatin based nanoparticles for controlled drug delivery applications has been cited in the literature.¹⁵⁻¹⁸

*For correspondence

Glutaraldehyde which is a synthetic crosslinker, has been used to crosslink different natural polymers like gelatin, chitosan, starch, etc.¹⁹ Different natural and synthetic crosslinkers are mainly used to control the release of drugs.²⁰⁻²³

Several reports have addressed the use of gelatin for drug delivery applications but hardly there are any report on using gelatin in combination with different nanomaterials like clay, metal oxides, CWs, etc. The inclusion of CWs may provide some important basis for further development in drug delivery applications. In this report, gelatin-CWs nanoparticles loaded with isoniazid drug were prepared by desolvation method followed by chemically crosslinked with glutaraldehyde. Also, the effect of CWs on gelatin nanoparticles in terms of their swelling and release behavior in different mediums, cytotoxicity, etc., have been studied.

2. Experimental

2.1 Materials

The natural polymer, gelatin type B 75 bloom from bovine skin and isoniazid drug were purchased from Sigma-Aldrich Inc., USA. Histopaque 1077, and [3-(4, 5 dimethylthiazol-2-yl)-2,5-diphenyltetrazolium bromide] (MTT) were bought from Sigma-Aldrich Inc., Germany. Ordinary filter paper for preparation of cellulose whiskers (CWs) was purchased from local supplier. Tween 80 and glutaraldehyde (25%) were obtained from E-Merck, India. RPMI 1640 and fetal bovine serum (FBS) was purchased from HiMedia Laboratories, Mumbai, India. The rest of the chemicals used were of analytical grade.

2.2 Preparation of cellulose whiskers (CWs) from filter paper cellulose

Cellulose whiskers were prepared from paper cellulose by modifying the process as mentioned by Zhang *et al.*²⁴ Initially, the cellulose fibers were processed from filter paper by rubbing it continuously through a sieve plate equipped with a 100-mesh screen. The obtained cellulose was transferred into 200 mL of 3 M NaOH solution and warmed up to 70°C for 3 h. The fiber slurry was then filtered and washed with distilled water until the wash water was of neutral pH. The resulting fibers were air-dried and then transferred to 200 mL of DMSO warmed up to 70°C in a water bath for 3 h. Again, the resulting cellulosic fibers were filtered, washed three times with distilled water and finally air-dried. After that, the pretreated fibers were dispersed into an acidic aqueous solution containing

100 mL of mixed acid (10 mL of 12.1 N HCl, 30 mL of 36 N H₂SO₄ and 60 mL of distilled water). This mixture was heated at 70–80°C for 8 h in a three necked round bottom flask with a mechanical stirrer under vigorous stirring. After the hydrolysis process, ultrasonication of the nano-sized cellulose dispersed in water was done for 30 min. It was followed by centrifugation at 4000 rpm for 15 min and finally washed with distilled water until pH of the supernatant was nearly 7. Afterwards, ultrasonication of the nano-sized cellulose dispersed in water was continued for 30 min and finally freeze dried.

2.3 Preparation of isoniazid loaded gelatin-CWs nanoparticles

Isoniazid-loaded gelatin-CWs nanoparticles were prepared by desolvation method (Figure 1) as reported in the literature with modifications.²⁵ 1% (w/v) gelatin solution was prepared in distilled water in a beaker and stirred with a magnetic stirrer for 30 min. Then, the varying percentage of CWs (1–7% w/w of gelatin) which were dispersed in water and sonicated for 30 min, was added to the gelatin solution under stirring condition. Then, 0.01 mL of tween 80 and isoniazid drug (0.01 g) were added to the mixture under stirring. Then, 50 mL of acetone was added for completely desolvating and precipitating the gelatin-CWs nanoparticles. The temperature of the mixture was slowly kept down to 4°C. After that, constant amount of glutaraldehyde was added drop by drop as cross-linker to crosslink the nanoparticles. The temperature of the mixture was increased slowly up to 45°C and stirring was continued for 1 h. Then, the cross-linked product was cooled, centrifuged and finally vacuum dried to obtain the isoniazid loaded gelatin-CWs nanoparticles.

A series of different crosslinked isoniazid loaded gelatin-CWs nanoparticles were prepared for the current study as represented in Table 1.

2.4 Calibration curve of isoniazid

A calibration curve was calculated for the measurement of release rate of isoniazid drug from the gelatin-CWs nanoparticles as reported in the literature.²⁶ A known concentration of the isoniazid drug in double distilled water was studied in the range of 200–600 nm using UV-Visible spectrophotometer (UV-2001 Hitachi, Tokyo, Japan). A prominent peak at 262 nm was observed for isoniazid having concentration within the range of 0.001–0.01g/100mL. Series of drug samples having different isoniazid concentration were prepared and their absorbance values at 262 nm were recorded and plotted. Then, the unknown concentration

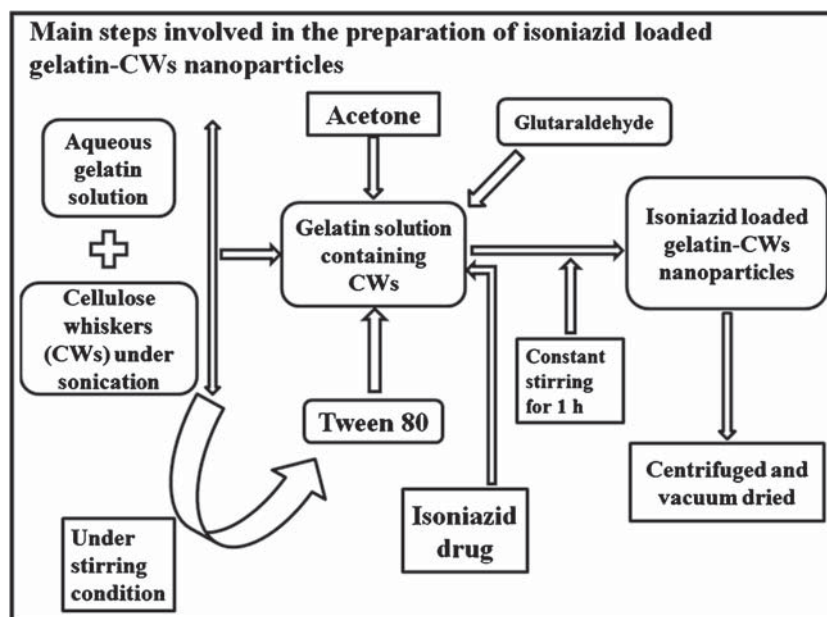


Figure 1. Flowchart diagram showing the main steps involved in the preparation of isoniazid loaded gelatin-CWs nanoparticles.

Table 1. Formulations for the preparation of different crosslinked isoniazid loaded gelatin-CWs nanoparticles.

Sample code	Gelatin (g) (in 100 mL water)	Isoniazid drug (g)	CWs (%) (w/w) w.r.t. gelatin (g)	GA (%) (v/w) w.r.t. gelatin (mL)	Tween 80 (mL)	Acetone (mL)
G1/CW0/GA1	1	0.01	0 (0.00)	1 (0.01)	0.01	50
G1/CW1/GA1	1	0.01	1 (0.01)	1 (0.01)	0.01	50
G1/CW3/GA1	1	0.01	3 (0.03)	1 (0.01)	0.01	50
G1/CW5/GA1	1	0.01	5 (0.05)	1 (0.01)	0.01	50
G1/CW7/GA1	1	0.01	7 (0.07)	1 (0.01)	0.01	50

of isoniazid drug was calculated using the calibration curve. Finally, the cumulative release (%) was calculated from the calibration curve by examining the amount of drug released at different media.

2.5 Calculation of isoniazid drug loading and encapsulation efficiency (EE) of the gelatin-CWs nanoparticles

The different formulations of the nanoparticles were centrifuged at room temperature for 15 min for calculating the drug loading and encapsulation efficiency of the nanoparticles. The amount of free isoniazid was measured from the supernatant liquid at 262 nm.²⁷

Encapsulation efficiency (%) and drug loading efficiency (%) can be calculated using the following equations.

$$\text{Encapsulation efficiency (EE) (\%)} = \frac{(\text{Total amount of isoniazid} - \text{Free amount of isoniazid})}{\text{Weight of dry nanoparticles}} \times 100$$

$$\text{Loading efficiency (LE) (\%)} = \frac{(\text{Total amount of isoniazid} - \text{Free amount of isoniazid})}{\text{Total amount of drug}} \times 100$$

2.6 Calculation of process yield (%)

Process yield (%) was calculated by using the following equation as cited in the literature.⁴

$$\text{Process Yield (\%)} = \frac{[(\text{Weight of nanoparticles} \times 100)]}{[\text{Weight of (isoniazid + CWs + gelatin)}]}$$

2.7 Characterization

FTIR spectroscopy was performed to study the interaction between gelatin, isoniazid and CWs. The samples were ground, mixed with KBr and finally compressed under vacuum. The spectra were recorded in the range of 4000–400 cm⁻¹ using FTIR spectrophotometer

(Nicolet, impact-410, USA). The distribution of isoniazid in gelatin-CWs nanoparticles was studied by X-ray diffractometry (Rigaku X-ray diffractometer, Miniflux, UK) using $\text{CuK}\alpha$ radiation with a scanning rate of 1°min^{-1} at an angle of $2\theta = 2-70^\circ$. The surface morphologies of isoniazid loaded gelatin-CWs nanoparticles were examined by a scanning electron microscope (JEOL JSM – 6390LV) with an acceleration voltage of 15 kV. The dispersion of CWs in the gelatin nanoparticles was studied by a Transmission Electron Microscope (FEI TECHNAI G2 20 S-TWIN) at an acceleration voltage of 200 kV. Particle size was analyzed by a dynamic light scattering (DLS) analyzer (Model DLS—Nano ZS, Zetasizer, Nanoseries, Malvern Instruments).

2.8 Swelling studies

The swelling study of isoniazid loaded gelatin-CWs nanoparticles was performed in two different buffer systems of pH 1.2 (0.1 N HCl) and pH 7.4 (phosphate buffer) for different time periods (1-8 h). For that purpose, weight of the dry nanoparticles were taken in filter paper pouches and immersed into two buffer solutions of either pH 1.2 or 7.4. At predetermined time interval, they were taken out from the buffer medium and blotted with ordinary filter paper to eliminate the excess swelling medium from the surface and finally weight of the swollen nanoparticles after definite time period was taken.²⁸ The swelling experiment was performed in triplicate and presented as mean value.

The percentage of swelling was determined as,

$$S(\%) = [(W_1 - W_2)/W_2] \times 100$$

where, W_1 = weight of swollen nanoparticles and W_2 = weight of dry nanoparticles before swelling.

2.9 *In vitro* release studies

To determine the release profile for the isoniazid loaded gelatin-CWs nanoparticles, accurately weighed samples were dipped into a solution of two different buffer systems of pH 1.2 and pH 7.4. They were first taken in pouches made from filter paper and placed in the buffer medium. After scheduled time interval, 5 mL solution was withdrawn from the medium and at the same time equal amount of the same solution was returned to keep the constant volume. The absorbance values for the different samples were recorded at 262 nm and finally the cumulative release (%) was calculated from the calibration curve.⁴

2.10 Isolation of lymphocytes, culture and treatment

Cytotoxicity of the isoniazid drug, gelatin and also gelatin-CWs nanoparticles were calculated using *in vitro*

cultured isolated human lymphocytes. Human blood was collected and diluted into the ratio of 1:1 using phosphate buffer saline (PBS) and 6 mL into 6 mL histopaque was layered. The isolation of human lymphocytes and also the cell viability study were performed as per the procedure cited in the literature.²⁹ Cell viability was determined by Trypan blue exclusion method using a hemocytometer.³⁰ Aliquots of 200 μL of isolated cells were cultured in Roswell Park Memorial Institute medium (RPMI) along with 10% heat inactivated Fetal Bovine Serum (FBS). Initially, the cells were kept for 4 h in RPMI without FBS in 5% CO_2 at 37°C in an incubator. Cells were then maintained as per requirements and finally treated in presence of FBS for 8 h.

2.11 Cytotoxicity study

By performing the cytotoxicity study, cell viability was calculated according to the method as reported in the literature.³¹ In this report, DMSO was used as the control solvent. The yellow color component of (3-[4,5-dimethylthiazol-2-yl]-2,5-diphenyl tetrazolium bromide) (MTT) turned into purple insoluble formazan crystals on treatment with viable cells. Then, the resulting purple color solution was measured using a UV-Visible spectrophotometer. The degree of cytotoxicity was determined by the amount of formazan crystals formed resulting from increase or decrease in cell number. Briefly, after treatment, cells were preserved with 10% MTT for 2 h. Then, the formazan crystals were dissolved in solvent and finally the absorbance value of the solution was determined at 570 nm. The absorbance of control cells at 8 h was established as 100% viability and the values of the treated cells were studied as the control percentage.

2.12 Statistical analysis

All the data were presented as mean \pm SD. The results were statistically analyzed by Student's t-test using a Graph Pad software (GraphPad Software Inc., California, USA).³² The significant difference between the control and the experimental group was set at different levels as $p < 0.05$, $p < 0.01$ and $p < 0.001$.

3. Results and Discussion

3.1 X-ray diffraction studies

The XRD diffractograms of the ground filter paper, CWs, gelatin, isoniazid and isoniazid loaded gelatin-CW

nanoparticles are shown in Figure 2. CWs showed diffraction peaks at $2\theta = 14.67^\circ$, 22.38° and 34.4° corresponding to the (1-10), (002), and (004) crystallographic planes, respectively (Figure 2d).³³ However, the intensities of the peaks (Figure 2d) at $2\theta = 14.67^\circ$ and 22.38° appeared much sharper than those of ordinary filter paper cellulose (Figure 2c) indicating the increase in crystallinity due to conversion of filter paper

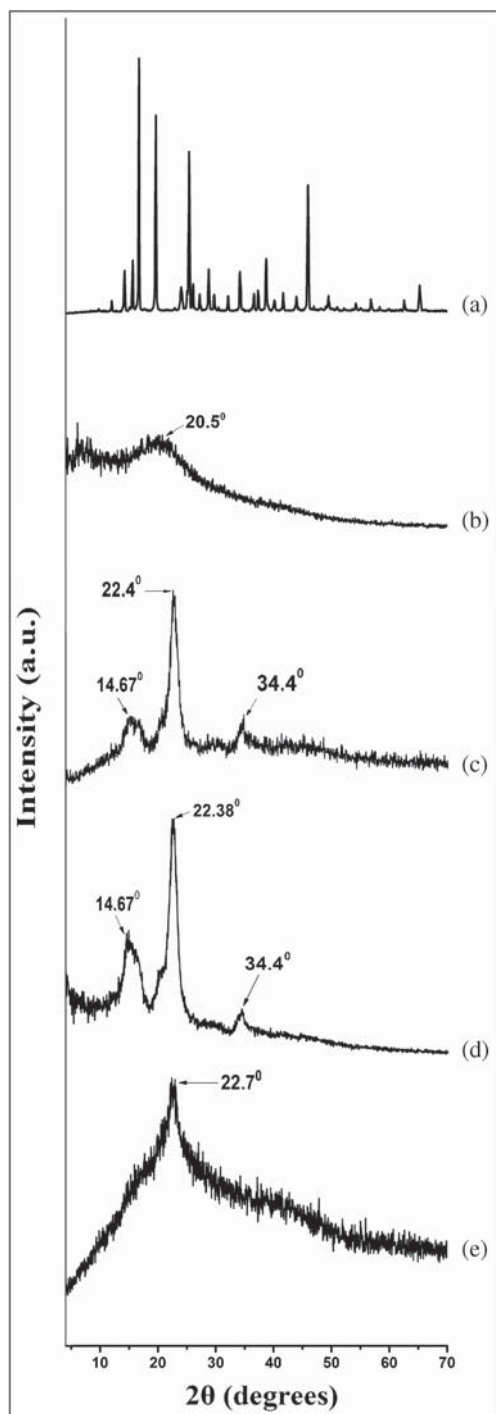


Figure 2. XRD graphs of (a) isoniazid drug, (b) gelatin, (c) filter paper cellulose (d) CWs, and (e) G1/CW5/GA1.

cellulose to CWs.³³ Again, in the diffractogram of isoniazid drug, multiple sharp peaks were obtained at $2\theta = 12-50^\circ$ indicating its highly crystalline nature. Similar type of diffractogram was reported by Maji *et al.*³⁴ On the other hand, gelatin (Figure 2b) showed its characteristic diffraction peak at $2\theta = 20.5^\circ$ corresponding to the (100) plane which indicated its amorphous nature.³⁴ In the diffractogram of isoniazid loaded gelatin-CWs nanoparticles, one sharp peak at $2\theta = 22.7^\circ$ was noticed indicating the incorporation of CWs into the nanoparticles. However, the absence or decrease in intensity of the other peaks indicated the loss in structure of CWs into the nanoparticles. It might be either due to the vigorous mixing or due to the presence of gelatin matrix.³³ The disappearance of characteristic peaks (Figure 2e) of isoniazid in the gelatin-CWs nanoparticles suggested the molecular level dispersion of isoniazid into the nanoparticles.³⁵

3.2 FTIR studies

From the FTIR spectrum of filter paper cellulose (Figure 3b), a broad peak was observed at 3433 cm^{-1} which is due to -OH stretching. The peak observed at 2899 cm^{-1} is attributed to symmetric -CH stretching. A strong band was observed at 1646 cm^{-1} which is attributed to stretching vibration of H-O-H intermolecular linkages. Two peaks at 1436 cm^{-1} and 1323 cm^{-1} are attributed to symmetric -CH₂ bending and wagging, respectively. One strong peak was observed at 1369 cm^{-1} which was due to C-H bending vibration. Peaks at 1164 cm^{-1} and 894 cm^{-1} are attributed to C-O-C stretching frequency at the β -(1 \rightarrow 4) glycosidic linkages. A small peak at 1105 cm^{-1} is due to the in-plane ring of the β -(1 \rightarrow 4) glycosidic linkages. The peak at 1059 cm^{-1} is assigned to the C-O stretching at C-3. Also, two peaks observed at 670 cm^{-1} and 597 cm^{-1} are the characteristic absorption of cellulose I α and I β , respectively.³³ The spectrum of CWs (Figure 3c) showed the presence of all the significant peaks for ground filter paper, but some changes were observed in the intensities of the peaks. The intensities of the same peaks appeared at 1369 cm^{-1} , and 896 cm^{-1} increased whereas the intensities of the peaks found at 2899 cm^{-1} , 1646 cm^{-1} and 1323 cm^{-1} decreased slightly. This suggested that some modifications took place due to conversion of filter paper cellulose to CWs. From the FTIR spectrum, it was observed that the absorption peaks for gelatin (Figure 3a) appeared at 3410 cm^{-1} for NH-stretching, 1639 cm^{-1} for amide-I, -CO and -CN stretching, 1566 cm^{-1} for amide-II and 1260 cm^{-1} for amide-III, respectively. Among all the absorption bands, the amide-I band observed at 1639 cm^{-1} is the most important peak for IR analysis of

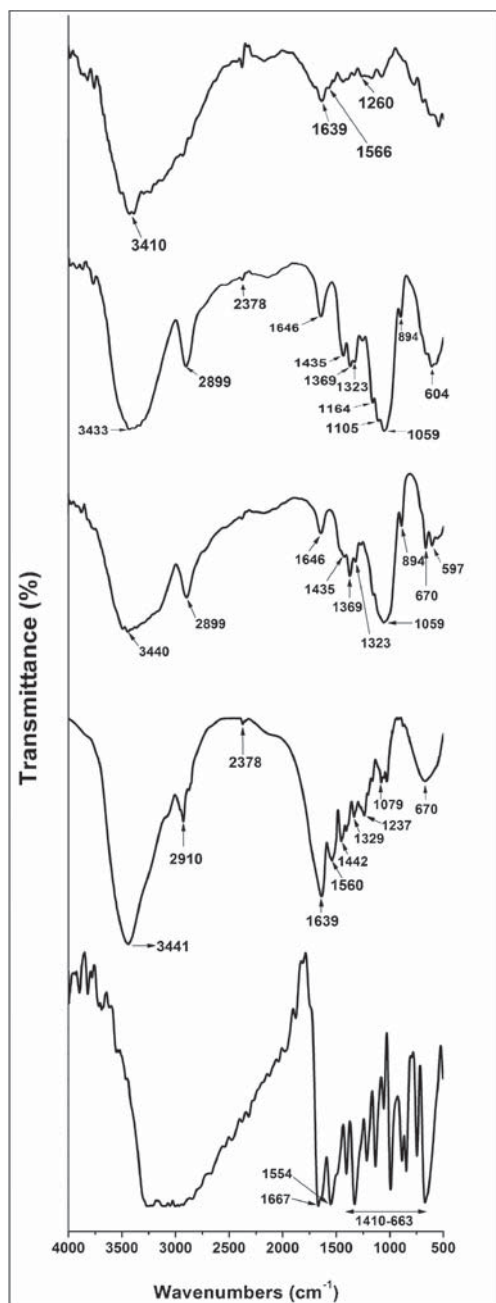


Figure 3. FTIR spectra of (a) gelatin, (b) filter paper cellulose, (c) CWs, (d) G1/CW5/GA1 and (e) isoniazid drug.

gelatin.^{34,36} In the spectrum of isoniazid (Figure 3e), the peak observed at 1667 cm^{-1} for amide-I is due to $\text{C}=\text{O}$ stretching. Also, the peak appeared at 1554 cm^{-1} for amide-II is attributed to N-H bending of the secondary amide group. Also, multiple peaks were observed in the isoniazid spectrum in between $1410\text{--}663\text{ cm}^{-1}$.²⁷ All the characteristic peaks of isoniazid, CWs and gelatin appeared and their intensities decreased in the spectrum of isoniazid loaded gelatin nanoparticles (Figure 3d) indicating the successful loading of isoniazid into the nanoparticles.

3.3 SEM analysis

SEM analysis was performed to study the surface morphology of filter paper cellulose, CWs, gelatin nanoparticles without CWs and isoniazid loaded gelatin-CW nanoparticles. From Figure 4a, it is seen that the surface of the untreated filter paper cellulose looked a little bit irregular and agglomerated. The surface of the CWs was found to appear as small rod-like shape and agglomerated.³⁷ In both Figure 4c and 4d, particles showed spherical shape but the surface of isoniazid loaded gelatin-CW nanoparticles (Figure 4d) appeared a little bit rougher than that of gelatin nanoparticles without CWs (Figure 4c) indicating good adherence of CWs with the gelatin matrix.

3.4 TEM analysis

TEM micrographs of isoniazid loaded gelatin nanoparticles without and with CWs are shown in Figures 5a and 5b, respectively. In Figure 5a, particles are seen as spherical in shape though agglomerated. Figure 5b shows the presence of network structure of CWs in the gelatin matrix. CWs chains are bundled together due to the formation of hydrogen bonding between the CWs and the gelatin matrix. This type of structures are absent in Figure 5a. The results indicated that the CWs were successfully incorporated and dispersed into the gelatin matrix. Similar types of findings were reported by Maji et al.³³

3.5 Effect of variation of concentration of CWs on the different properties of gelatin nanoparticles

The results showing the effect of the variation of concentration of CWs on the different properties of gelatin nanoparticles are shown in Table 2. Both encapsulation efficiency (%) and drug loading efficiency (%) were found to be higher in the case of CWs containing crosslinked gelatin nanoparticles. Both encapsulation efficiency (%) and drug loading efficiency (%) decreased with the increase in content of CWs. It might be due to the presence of network structure of CWs which resists the diffusivity of drug molecules into the gelatin nanoparticles. Moreover, the $-\text{OH}$ group of CWs might have interacted with $-\text{NH}_2$ groups of gelatin and $-\text{CHO}$ groups of glutaraldehyde (GA) resulting in extension of the polymer matrix. The network structure of CWs which created a tortuous path, restricted the free movement of the intercalated polymer chains. Hence, encapsulation efficiency (%) and drug loading efficiency (%) decreased. But, variation of CWs content did not produce much influence on process yield (%) which were obtained above 80% for all samples.

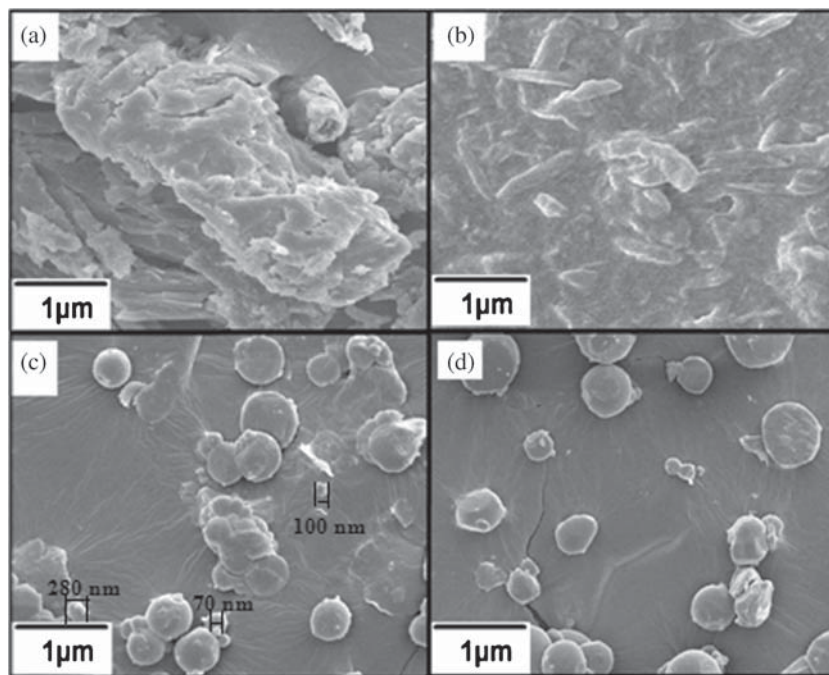


Figure 4. SEM picture of (a) filter paper cellulose, (b) CWs, (c) G1/CW0/GA1, and (d) G1/CW5/GA1.

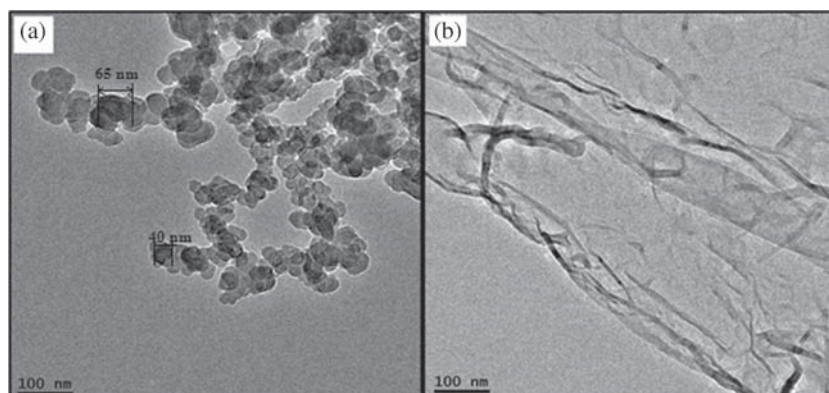


Figure 5. TEM picture of crosslinked isoniazid loaded gelatin nanoparticles (a) without CWs range and (b) with CWs.

The hydrodynamic size of crosslinked gelatin nanoparticles in aqueous medium was studied by DLS method.³⁸ Particle size distribution curve for a typical sample (G1/CW0/GA1) is shown in Figure 6. The average particle size is 313.2 ± 15 nm. Similarly, the

hydrodynamic size of other nanoparticles was measured by Dynamic Light Scattering (DLS) study and given in Table 2. CWs containing nanoparticles exhibited higher size compared to those of CWs-free nanoparticles. The extended polymer chain structure caused

Table 2. Effect of variation of concentration of CWs on the different properties of isoniazid loaded gelatin nanoparticles.

Sample code	Process Yield (%)	Encapsulation efficiency (EE) (%)	Loading efficiency (%)	Average diameter from DLS study (nm)	Zeta potential (mV)
G1/CW0/GA1	82.45 (± 0.08)	62.56 (± 0.04)	24.45 (± 0.04)	313.2 (± 15)	-21.1 (± 0.01)
G1/CW1/GA1	89.23 (± 0.01)	61.01 (± 0.03)	22.66 (± 0.09)	745.4 (± 8)	-19.3 (± 0.03)
G1/CW3/GA1	90.67 (± 0.01)	58.39 (± 0.01)	22.06 (± 0.02)	363.6 (± 12)	-18.8 (± 0.01)
G1/CW5/GA1	83.25 (± 0.04)	58.03 (± 0.03)	20.49 (± 0.02)	404.2 (± 4)	-13.2 (± 0.01)
G1/CW7/GA1	82.56 (± 0.03)	52.68 (± 0.01)	18.23 (± 0.04)	442.5 (± 7)	-10.7 (± 0.06)

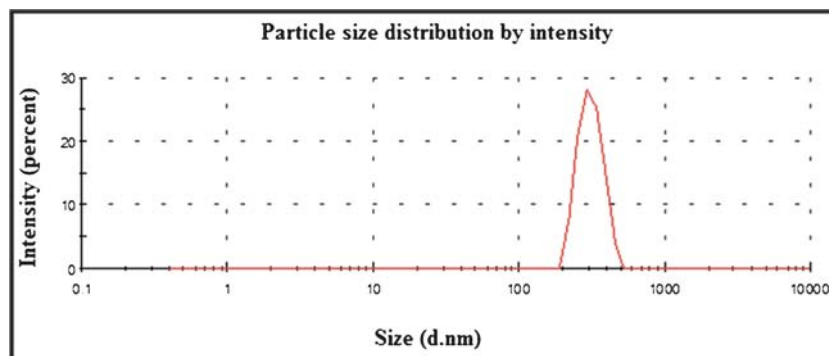


Figure 6. Particle size distribution curve of G1/CW0/GA1.

by the interaction as stated earlier might be responsible for this. The particle size distribution curves for other samples are given in Supplementary Information files (SI).

The variations in the particle size distribution inferred from the different microscopies and light scattering experiments are likely to be due to the difference in the mode of operation involved in the imaging processes, and inherent assumptions made in the particle size analysis protocols.

Zeta potential values of the crosslinked gelatin nanoparticles were found in the range of -10.7 to -21.1 mV. The surface of the nanoparticles was found to be negatively charged. The zeta potential values were found to be decreased with the increase in CWs content. The decrease in surface charge might be due to increase in electrostatic interaction between the protonated amino groups of gelatin matrix and $-OH$ groups of CWs.

3.6 Swelling study

The effect of CWs on swelling degree (%) of crosslinked gelatin nanoparticles loaded with isoniazid in two buffer systems at pH 1.2 and 7.4 are shown in Figure 7. From the corresponding curves, it was observed that swelling (%) increased with time. With increase in time, higher amount of solvent might have entered into the gelatin matrix and as a result swelling (%) increased. Again, swelling (%) was found to be more at pH 7.4 than at pH 1.2. It might be due to the fact that at pH 7.4, the gelatin molecules contain a negative charge due to the presence of $-COO^-$ groups in the molecule. As a result, at pH 7.4, the completely ionized isoniazid molecules interacted with those of negatively charged centers present at the gelatin molecules, and hence, swelling (%) increased.³⁹

Moreover, swelling degree (%) was found to decrease with increase in content of CWs. It might be due to the fact that the presence of dispersed phase at CWs

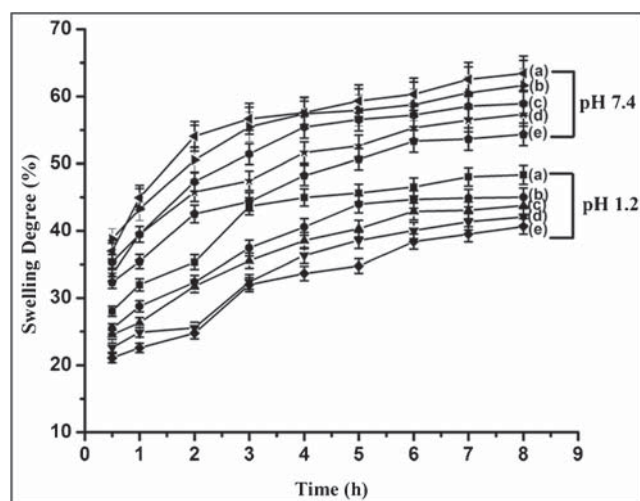


Figure 7. Swelling degree (%) vs. time plots of isoniazid loaded gelatin-CWs nanoparticles at pH 7.4 and at pH 1.2 of (a) G1/CW0/GA1, (b) G1/CW1/GA1, (c) G1/CW3/GA1, (d) G1/CW5/GA1, and (e) G1/CW7/GA1.

decreased the water absorption into the gelatin matrix. CWs provided a tortuous path which restricted the diffusivity of water molecules through the gelatin nanoparticles and hence swelling (%) decreased.³³

3.7 Drug release study

Figure 8 shows the drug release behavior of crosslinked gelatin nanoparticles prepared by varying the percentage of CWs at pH 1.2 and 7.4. From both the curves of Figure 8, cumulative release (%) of the isoniazid drug was found to increase with time. The release was found to be higher at basic pH than at acidic pH throughout the time duration. This might be due to the fact that when isoniazid-loaded gelatin nanoparticles were placed in the release medium, $-COO^-$ groups of gelatin molecules repelled each other, hence produced a better relaxation in the gelatin-CWs nanoparticles. This resulted in greater swelling of the gelatin nanoparticles

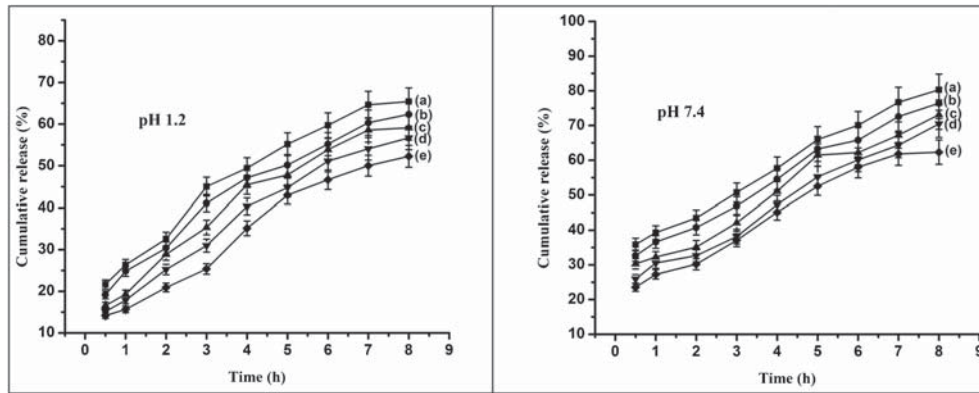


Figure 8. Effect of variation of concentration of CWs on the cumulative release (%) of isoniazid from gelatin-CW nanoparticles at pH 1.2 and pH 7.4. (a) G1/CW0/GA1, (b) G1/CW1/GA1, (c) G1/CW3/GA1, (d) G1/CW5/GA1, and (e) G1/CW7/GA1.

which, in turn, produced greater release of the isoniazid drug from gelatin-CWs nanoparticles.³⁹

On the other hand, cumulative release (%) of isoniazid drug was found to decrease with increase in

CWs content (Figure 8). This might be due to decrease in swelling with increase in CWs content in which, the solvent molecules could not diffuse out properly to attach with the isoniazid molecules loaded in the

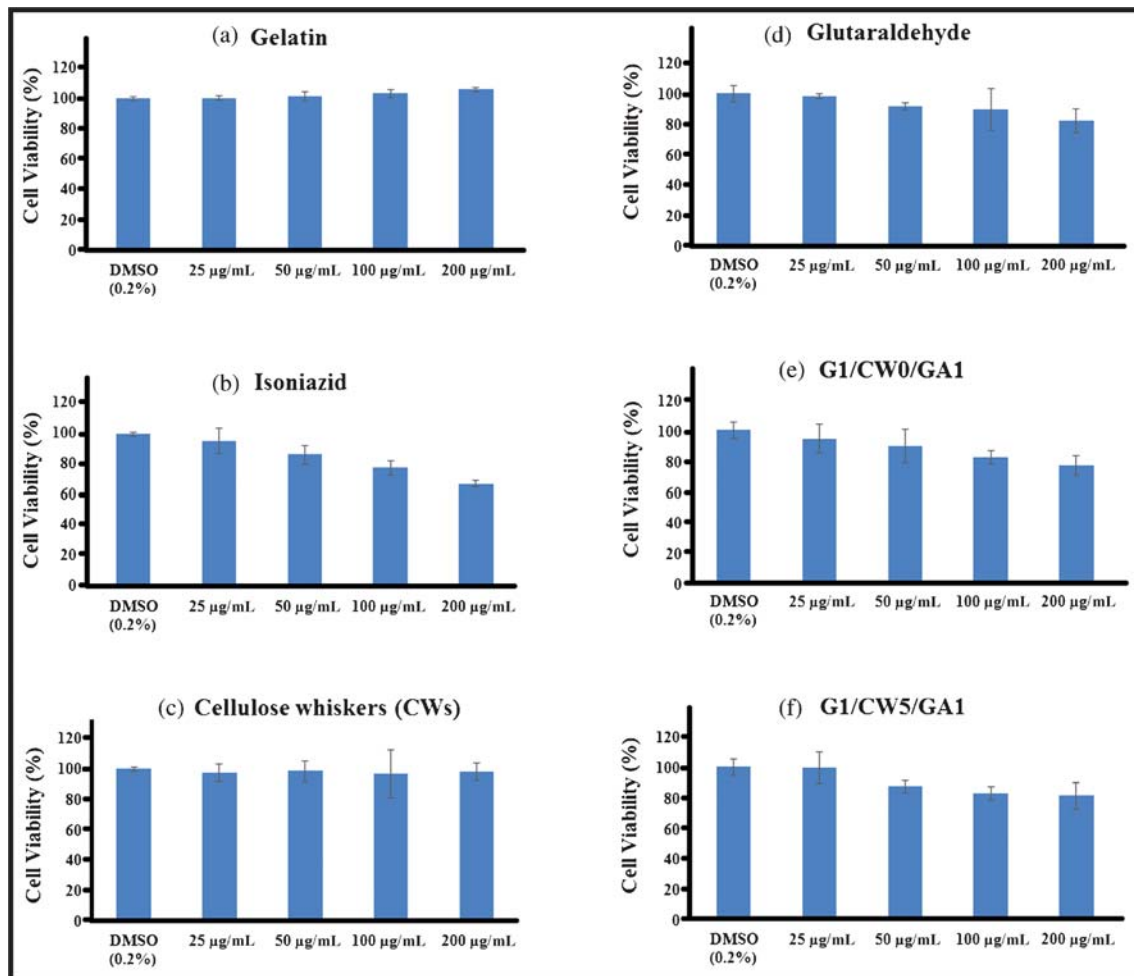


Figure 9. Cytotoxicity study of (a) gelatin, (b) isoniazid, (c) CWs, (d) glutaraldehyde, (e) G1/CW0/GA1, and (f) G1/CW5/GA1.

gelatin nanoparticles. Actually, CWs can regulate the swelling and release behavior of the drug. On the contrary, if gelatin is used alone for loading of the drug, then swelling and release properties will be hampered and quick release of the drug will take place. The controlling of swelling and release of drug in loaded gelatin nanoparticles will be in narrow range whereas the incorporation of CWs into gelatin matrix will broaden the controlling range. Also, the swelling degree (%) increased with increase in time so, more and more solvent molecules could attach the drug molecules assisting more release of the drug from the gelatin nanoparticles.

3.8 Cytotoxicity test

The results of MTT assay in human lymphocytes are shown in Figure 9. MTT assay was done for different components and different concentrations of nanoparticles at 8 h. From the Figure 8a, it is seen that gelatin showed around 100% cell viability indicating its non-toxic nature to human lymphocytes. The prepared CWs sample was found to be cell compatible and showed almost 98% of cell viability (Figure 9c). CWs sample is not toxic to human lymphocytes since it was prepared from cellulose. Similar findings were reported by Clift *et al.*⁴⁰ Again, cytotoxicity study showed that isoniazid and glutaraldehyde alone were toxic to human lymphocytes (Figure 9b and 9d). Isoniazid showed only 60% of cell viability and thus highly cytotoxic to cells (Figure 9b). Isoniazid is a synthetic anti-tuberculosis drug and it shows higher toxicity to human lymphocytes (Figure 9b) when used alone due to its high availability to cells. The delivered drug should be between the maximum value, which may represent a toxic level, and a minimum value, below which drug is no longer effective. In the absence of gelatin coating, the level of drug rises, crossing the maximum level in blood, making it toxic after each administration and then decreases below the minimum level and making it ineffective. Therefore, the drug has to be administered at a regular interval in order to keep the drug level constant in the blood. In controlled delivery application, repeated administration of drug is not necessary. The function of gelatin is to control the release of drug. Hence, isoniazid-loaded gelatin nanoparticles slowed down the release of amount of isoniazid at a particular time and made it less toxic to the cells. It was also observed that gelatin-CWs nanoparticles showed more cell viability (%) than CWs-free gelatin nanoparticles. The drug diffused out slowly due to the network structure of CWs, and could interact slowly with cells and hence increase in cell viability (%).

4. Conclusions

Cellulose Whiskers (CWs) were prepared from filter paper cellulose by acid hydrolysis. Also, gelatin-CW nanoparticles loaded with isoniazid were successfully prepared by desolvation method using glutaraldehyde as chemical crosslinker. XRD studies showed the increase in crystallinity of the CWs compared to filter paper cellulose and also showed molecular level dispersion of isoniazid into the gelatin nanoparticles. XRD and TEM study showed the successful incorporation of CWs into the gelatin matrix. FTIR studies showed the incorporation of isoniazid and CWs into the gelatin nanoparticles. The rod-like shape of CWs and smooth surface of gelatin-CWs nanoparticles were observed as revealed by SEM study. Both swelling degree (%) and cumulative release (%) were found to increase with the increase in time and also found to be higher in basic medium. Swelling degree (%) and cumulative release (%) were also found to decrease with the increase in CWs content. Cytotoxicity study indicated that CWs were non-toxic to human lymphocytes and also gelatin nanoparticles containing CWs were less toxic than CWs-free nanoparticles. The results suggested that gelatin-CWs nanoparticles have potential applications in controlled drug delivery.

Supplementary Information (SI)

All additional information regarding particle size distribution analysis of isoniazid loaded gelatin-CWs nanoparticles using DLS technique (Figures S1, S2, S3 and S4) are given in the supporting information available at www.ias.ac.in/chemsci.

References

1. Uhrich K E, Cannizzaro S M, Langer R S and Shakesheff K M 1999 *Chem. Rev.* **99** 3181
2. Pillai O and Panchagnula R 2001 *Curr. Opin. Chem. Biol.* **5** 447
3. Harisha R S, Hosamani K M, Keri R S, Shelke N, Wadi V K and Aminabhavi T M 2010 *J. Chem. Sci.* **122** 209
4. Devi N and Maji T K 2009 *AAPS Pharm. Sci. Tech.* **10** 1412
5. Lee E J, Khan S A, Park J K and Lim K H 2012 *Bioprocess Biosyst. Eng.* **35** 297
6. Dash R and Ragauskas A J 2012 *RSC Adv.* **2** 3403
7. Ljungberg N, Cavaille J Y and Heux L 2006 *Polymer* **47** 6285
8. Bendahou A, Kaddami H and Dufresne A 2010 *Eur. Polym. J.* **46** 609
9. Abeer M M, Amin M C I M and Martin C 2014 *J. Pharm. Pharmacol.* **66** 1047
10. Haywood A, Mangan M, Grant G and Glass B D 2005 *J. Pharm. Pract. Res.* **35** 181

11. Cheng J, Teply B A, Jeong S Y, Yim C H, Ho D, Sherifi I, Jon S, Farokhzad O C, Khademhosseini A and Langer R S 2006 *Pharm. Res.* **23** 557
12. Degim I T and Celebi N 2007 *Curr. Pharm. Des.* **13** 99
13. Zhang R, Song Z, Yin L, Zheng N, Tang H, Lu H, Gabrielson N P, Lin Y, Kim K and Cheng J 2015 *WIREs Nanomed. Nanobiotechnol.* **7** 98
14. Jahanshahi M and Babaei Z 2008 *Afr. J. Biotechnol.* **7** 4926
15. Foox M and Zilberman M 2015 *Expert Opin. Drug. Deliv.* **12** 1547
16. Azimi B, Nourpanah P, Rabiee M and Arbab S 2014 *Iran. Biomed. J.* **18** 34
17. Kaintura R, Sharma P, Singh S, Rawat K and Solanki P R 2015 *J. Nanomed. Res.* **2** 00018 doi:10.15406/jnmr.2015.02.00018
18. Saraogi G K, Sharma B, Joshi B, Gupta P, Gupta U D, Jain N K and Agrawal G P 2011 *J. Drug Targeting* **19** 219
19. Whipple E B and Ruta M 1974 *J. Org. Chem.* **39** 1666
20. Xu H, Shen L, Xu L and Yang Y 2015 *Biomed. Microdevices* **17** 8
21. Zheng J P, Luan L, Wang H Y, Xi L F and Yao K D 2007 *Appl. Clay Sci.* **36** 297
22. Song F, Zhang L M, Yang C and Yan L 2009 *Int. J. Pharm.* **373** 41
23. Hosseinzadeh H 2010 *J. Chem. Sci.* **122** 651
24. Zhang J, Elder T J, Pu Y and Ragauskas A J 2007 *Carbohydr. Polym.* **69** 607
25. Ramachandran R and Shanmughavel P 2010 *Indian J. Biochem. Biophys.* **47** 56
26. Devi N and Maji T K 2010 *Drug Dev. Ind. Pharm.* **36** 56
27. Selvaraj S, Saravanakumar N, Karthikeyan J, Deborah D E and Rajendran N N L 2010 *Der Pharmacia Lettre* **2** 420
28. Cassano R, Trombino S, Ferrarelli T, Mauro M V, Giraldo C, Manconi M, Fadda A M and Picci N 2012 *J. Biomed. Mater. Res. A* **100** 536
29. Hussain A, Saikia V and Ramteke A 2012 *Free Rad. Antiox.* **2** 8
30. Gomez-Lechon M J, Iborra F J, Azorin I, Guerri C and Renau-Piqueras J 1992 *Methods Cell. Sci.* **14** 73
31. Denizot F and Lang R 1986 *J. Immunol. Methods* **89** 271
32. Daly L E, Bourke G J and Mc Gilvray J 1985 In *Interpretation and Uses of Medical Statistics* (London: Blackwell Scientific Publications) p.41
33. Iman M, Bania K K and Maji T K 2013 *Ind. Eng. Chem. Res.* **52** 6969
34. Sarmah M, Banik N, Hussain A, Ramteke A, Sharma H K and Maji T K 2015 *J. Mater. Sci.* **50** 7303
35. Angadi S C, Manjeshwar L S and Aminabhavi T M 2010 *Int. J. Biol. Macromol.* **47** 171
36. Devi N and Maji T K 2011 *Int. J. Polym. Mater.* **60** 1091
37. Lu P and Hsieh Y 2010 *Carbohydr. Polym.* **82** 329
38. Sarmiento B, Ribeiro A, Veiga F, Sampaio P, Neufeld R and Ferreira D 2007 *Pharm. Res.* **24** 2198
39. Bajpai A K and Choubey J 2006 *J. Mater. Sci.: Mater. Med.* **17** 345
40. Clift M J D, Foster E J, Vanhecke D, Studer D, Wick P, Gehr P, Rothen-Rutishauser B and Weder C 2011 *Biomacromolecules* **12** 3666